Characterization of nanostructure in $Si_{1-x}Ge_x$ epilayers using x-ray reflectivity and fluorescence techniques

S. Kim,[a] G. Kioseoglou,[b] S. Huang, and Y. H. Kao
Department of Physics, State University of New York at Buffalo, Amherst, New York 14260

Y. L. Soo
Department of Physics, National Tsing Hua University, Hsinchu, Taiwan

X. Zhu and K. L. Wang
Electrical Engineering Department, University of California, Los Angeles, California 90024

(Received 29 April 2005; accepted 22 August 2005; published online 10 October 2005)

X-ray reflectivity and angular dependence of x-ray fluorescence (ADXRF) techniques are used for nondestructive characterization of nanostructure and interface morphology in a series of $Si_{1-x}Ge_x$ epilayers grown on Si by molecular-beam epitaxy. The ADXRF method is element specific, well suited for probing the depth profile of Ge in the system without disturbing the integrity of the material structure under study. The layer thickness, interfacial roughness, Ge concentration, lattice parameters, and x-ray optical constants for the entire series have been determined. The results show that the $Si_{1-x}Ge_x$ epilayers with x values between 0.27 and 0.83 are neither completely pseudomorphic nor fully relaxed. We have thus demonstrated that the reflectivity and ADXRF methods can be used as effective tools for studying various types of nanostructure in alloys. © *2005 American Institute of Physics*. [DOI: 10.1063/1.2073976]

I. INTRODUCTION

X rays from synchrotron radiation allow many useful approaches for nondestructive investigation of the atomic depth profile and morphology of *buried* interfaces in layer-structured materials. Utilizing the property that the x-ray penetration depth varies from nanometers to micrometers by changing the grazing incidence angle from below to above the critical angle of the material, the techniques of *x-ray reflectivity* and *angular dependence of x-ray fluorescence* (ADXRF) are particularly useful for studying the interface morphology and compositional profile without disturbing the integrity of the material structure under study. Moreover, the ADXRF method is element specific, hence well suited for probing the structure about selected atomic species in multi-element layered systems.

In general, the task of concentration depth profiling of layered materials involves (1) determination of the elemental concentration in the layers and (2) quantitative characterization of elemental intermixing or interdiffusion across the interfaces. Case (2) has already been demonstrated by using the x-ray reflectivity and ADXRF techniques with a series of CdS/CdTe heterojunctions[1] (where migration of the Te atoms and structural changes were studied) and a series of $CdS/Cu(In,Ga)Se_2$ heterojunctions[2] (where compositional intermixing at the rough surface was investigated). In this paper, case (1) along with variations in the interface morphology is demonstrated with a series of $Si_{1-x}Ge_x$ alloys.

Crystalline silicon-germanium ($Si_{1-x}Ge_x$) alloys have attracted considerable attention for both fundamental studies and technological applications due to their particularly useful electronic properties. These alloys can form solid solutions over the entire compositional range $0 \leqslant x \leqslant 1$; the possibility of continuous variation in the lattice parameter[3] as well as band gap[4] between Si and Ge affords a way to control the material properties for Si-related device applications. Silicon and germanium are in the diamond structure with lattice constants of 5.4309 and 5.6576 Å, respectively. Strain effects are naturally present in epitaxial growth of SiGe alloys on Si substrate due to the 4.2% lattice mismatch between Si and Ge. Various studies of strain effects and atomic structural changes due to the presence of an interface between $Si_{1-x}Ge_x$ and Si have been made in the past including the electronic properties,[5] critical layer thickness,[6–8] morphology of interfaces,[9] interatomic bond lengths,[10–13] and intermixing of elements across the interface,[14–16] providing a generally useful basis for exploring possible applications of the $Si_{1-x}Ge_x/Si$ epilayer junctions.

The distribution of constituent elements is a crucial factor which can affect the band structure in a strained $Si_{1-x}Ge_x$ epilayer. In the past, x-ray diffraction has been widely used to determine the composition based on an assumption of the well-known Vegard's law[17] that the lattice parameter of the solid solution is directly proportional to the atomic percent of solute present (i.e., the fraction x of Ge content). This assumption can only be justified when the system is a random solid solution. However, this traditional method for composition determination is unreliable in the present case for the following reasons. First, the thickness range of $Si_{1-x}Ge_x$ films of practical interest usually falls in the critical thickness range for various values of the Ge content x, and the alloy layer is often not *fully* relaxed and therefore at least partially strained. Second, even though the thickness of a $Si_{1-x}Ge_x$ layer may exceed the critical thickness, the residual inhomo-

[a]Present address: Experimental Diagnostic Imaging, University of Texas, M.D. Anderson Cancer Center, Houston, TX 77030.
[b]Present address: Naval Research Laboratory, Washington, DC 20375.

geneous strain is usually present in the alloy up to a large thickness range depending on the Ge content[18] and growth temperature.[19] Further, other currently available techniques for determining the composition in layered materials are inevitably detrimental or abrasive, making it difficult to reliably characterize the elemental distribution for as-made specimens and especially around the buried interface region. The development of *nondestructive* methods for atomic depth profiling of thin-film alloys containing strain would seem highly desirable.

The main purpose of the present paper is to demonstrate a useful application of the combined techniques of x-ray reflectivity and ADXRF for determining the interface morphology and Ge concentration in a series of $Si_{1-x}Ge_x$ epilayers grown on Si by molecular-beam epitaxy (MBE). The samples cover a large range of nominal Ge concentration x varying from 0.2 to 0.9 and some of these samples are either naturally or partially strained. So far no systematic studies of strained $Si_{1-x}Ge_x$ alloys with this wide range of Ge content variation have been reported. By the x-ray reflectivity method, the interfacial roughness and the layer thickness in this layer system have been determined. Using the geometrical parameters, the ADXRF method with its useful atomic selectivity allows an accurate determination of the Ge content in each sample, thus providing a way of nondestructive and quantitative calibration of the Ge concentration in the entire $Si_{1-x}Ge_x$ epilayer system.

II. BACKGROUND

When an electromagnetic wave impinges on a composite system containing layers of different materials each with a distinct refractive index, standing wave patterns are generated inside the layers due to interference between the transmitted waves and those reflected from the interfaces. From the angular dependence of the fluorescence intensity, information on the composition, thickness, and density of the thin layers can be obtained.[20,21] On the other hand, the measured reflectivity contains information on the layer thickness and interfacial roughness. Both the x-ray reflectivity and x-ray fluorescence intensity can be analyzed in terms of the relevant physical parameters such as elemental composition, density, thickness, and roughness. It has been realized that ADXRF measurements are more sensitive to the distribution of elements (e.g., composition and/or diffusion) while x-ray reflectivity gives more direct information on the geometrical parameter such as thickness and roughness. Król *et al.*[22] and de Boer[20] reported theoretical calculations for the x-ray fluorescence intensity of layered materials by using a matrix formalism and recursion relation, respectively. In 1991, Weisbrod *et al.* described a procedure for quantitative determination of the physical parameters of the layers and performed verification tests of the technique[21] as well as instrument calibration. In 1993, van den Hoogenhof and de Boer[23] have proposed glancing-incidence x-ray analysis for obtaining detailed information of the layered materials. A brief review of the x-ray reflectivity and ADXRF methods is presented in the following.

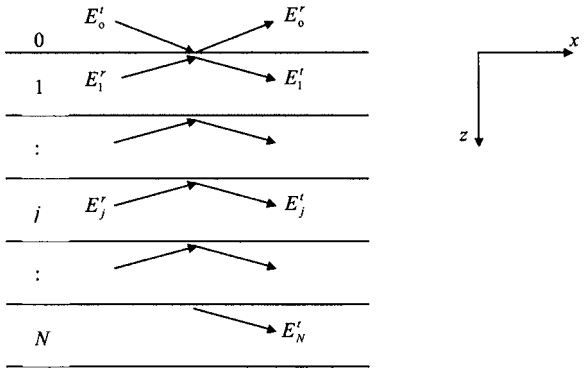

FIG. 1. A layer-structured system consisting of N layers. Vacuum and the substrate are labeled by 0 and N, respectively.

A. X-ray reflectivity

The effects of x rays on materials are commonly characterized by a complex refractive index $n=1-\delta-i\beta$, where both δ and β are of the order of 10^{-6}:

$$\delta=\frac{N_A}{2\pi}r_0\lambda^2\frac{\rho}{A}(Z+f'), \quad \beta=\frac{N_A}{2\pi}r_0\lambda^2\frac{\rho}{A}f''=\frac{\lambda}{4\pi}\mu, \tag{1}$$

where N_A is Avogadro's number, $r_0=e^2/mc^2$ the classical electron radius, λ the wavelength of x rays, ρ the mass density, A the atomic weight, Z the atomic number, μ the linear mass absorption coefficient, and f' and f'' are the anomalous scattering factors. For a multielement system, the optical constants δ and β are additive in terms of the weighted mass fractions.

The specular reflectivity for smooth surfaces can be analyzed by using the Parratt formalism.[24,25] Following the notations of de Boer,[20] we consider a layer-structured system consisting of N layers labeled $j=1,2,\ldots,N$, as shown in Fig. 1. In an idealized situation, if the interfaces are all so smooth that the effects due to interfacial roughness can be neglected, the coefficients of reflection r_j and transmission t_j at the jth interface [between the jth and $(j+1)$th layers] can then be obtained from the well-known Fresnel's formulas in optics:

$$r_j=(k_{z,j}-k_{z,j+1})/(k_{z,j}+k_{z,j+1}), \quad t_j=2k_{z,j}/(k_{z,j}+k_{z,j+1}), \tag{2}$$

where $k_{z,j}=k\sqrt{n_j^2-\cos^2\theta}$ is the z component of the wave vector in layer j, $k=2\pi/\lambda$ the modulus of the wave vector in vacuum (layer $j=0$), and θ the grazing angle of incidence. The transmitted field E_j^t and reflected field E_j^r at the interface j can be found from the recurrence relations:[20,24] $E_j^r=a_j^2X_jE_j^t$ and $E_{j+1}^t=a_j^2E_j^tt_j/(1+a_{j+1}^2X_{j+1}r_j)$, where $a_j=\exp(-id_jk_{z,j})$, d_j is the thickness of layer j, and X_j is expressed as $X_j=r_j+a_{j+1}^2X_{j+1}/1+a_{j+1}^2X_{j+1}r_j$ for $j=0,1,2,\ldots,N-1$. For a very thick substrate, $X_N=0$, since there is no need to consider the reflection occurring at its bottom. The specular reflectivity R is defined as the intensity ratio of the reflected beam and the incident beam:

$$R = \left| \frac{E_0^r}{E_0^t} \right|^2. \tag{3}$$

For a layered system with rough interfaces, a Gaussian probability density function[26,27] with a standard deviation σ_j (or simply *roughness*) is commonly assumed to represent the root-mean-square deviation σ_j of the jth interface height from a perfectly smooth plane such that

$$P_{\text{Gauss}}(z) = \frac{1}{\sqrt{2\pi}\sigma_j} e^{-z^2/2\sigma_j^2}. \tag{4}$$

It follows that the depth variation of the refractive index $n(z)$ between the jth and $(j+1)$th layers can be represented by an error function resulting from an integration over depth z of the density probability $P_{\text{Gauss}}(z)$ in this region:

$$n(z) = \frac{n_{j+1}+n_j}{2} + \frac{n_{j+1}-n_j}{2} \text{erf}\left(\frac{z}{\sqrt{2}\sigma_j} \right). \tag{5}$$

For the simple case of a multilayer system with sufficiently low interfacial roughness such that $\sigma_j |k_{jz}| < 1$, modified Fresnel's coefficients can be used approximately to account for the effects of interfacial roughness. The standard Fresnel's coefficients r_j and t_j can be conveniently replaced by $\tilde{r}_j = r_j \exp(-2k_{z,j}k_{z,j+1}\sigma_j^2)$ and $\tilde{t}_j = t_j \exp[(k_{z,j}-k_{z,j+1})^2\sigma_j^2]$ with the appearance of the Debye-Waller-like exponential factors in order to incorporate the effects of interfacial roughness.[26,28,29] In the hard x-ray regime, this "low roughness limit" approximation is only valid for multilayer systems with interfacial roughness σ_j values generally lower than about 50 Å. Otherwise, the phase relation between the incident and reflected beams is lost and hardly any specular reflection can take place.

B. ADXRF

Analysis of x-ray absorption is generally useful to account for the generation of x-ray fluorescence. The absorption of radiation is described by Poynting's theorem. The x-ray fluorescence intensity I_a (the number of photons emitted per unit area per unit time due to atoms of a selected element a), taking into account the absorption of radiation in the layer and neglecting the enhancement effects due to secondary fluorescence, can be expressed as[20]

$$I_a(\theta) \propto \int dz \left(-\frac{dS_z(\theta)}{dz} \right) \Phi_a(z) \exp\left(-\frac{\mu_a(z) z}{\sin \psi_d} \right), \tag{6}$$

where S_z is the z component (perpendicular to the sample surface) of the Poynting vector, $\Phi_a(z)$ the concentration depth profile of a specific atomic species a in the z direction, $\mu_a(z)$ the linear absorption coefficient of the considered fluorescence radiation from element a, and ψ_d the angle between detected fluorescence and sample surface. The concentration depth profile $\Phi_a(z)$ is given by $\Phi_a(z) = C_a(z)\rho(z)$, where C_a is the mass fraction of element a and ρ the material density. The last factor in the integrand of Eq. (6) accounts for the attenuation of the outgoing x-ray fluorescence from element a. The x-ray fluorescence intensity I_a of element a is proportional to the absorption of the incident x-ray beam by the sample $(-dS_z/dz)$ and the concentration of the element a (i.e., Φ_a). Quantitative determination of x-ray fluorescence intensity thus requires a detailed knowledge of the field distribution (in terms of layer parameters such as density, elemental composition, thickness, and roughness) convoluted with the concentration profile of the material in the layered structure.

The total energy flow and absorption within each layer of a multilayer system can be calculated using the results outlined above, and the x-ray fluorescence intensity as a function of the grazing incidence angle can therefore be derived. The total electric field $E_j(z)$ at depth z in layer j for s polarization can be expressed as the sum of the contribution due to radiation transmitted through the upper interface and the contribution due to radiation reflected from the bottom interface: $E_j(z) = E_j^t \exp(-ik_{z,j}z) + E_j^r \exp(ik_{z,j}z)$. The components of the Poynting vector can be found in terms of the electric fields E_j^t and E_j^r and the wave vector $k_{z,j}$ by using Maxwell's equation $\nabla \times \mathbf{E}_j = -\mu_0 \partial \mathbf{H}_j / \partial t$ (μ_0 is the vacuum permeability). Substitution of S_z in Eq. (6) and integration yields[20,30,31]

$$\begin{aligned} I_{aj} \propto C_{aj}\rho_j A_j \Bigg\{ & |E_j^t|^2 \frac{1-\exp[-(\mu_{aj}/\sin\psi_d + 2k''_{z,j})d_j]}{\mu_{aj}/\sin\psi_d + 2k''_{z,j}} \\ & + |E_j^r|^2 \frac{1-\exp[-(\mu_{aj}/\sin\psi_d - 2k''_{z,j})d_j]}{\mu_{aj}/\sin\psi_d - 2k''_{z,j}} \\ & + 2\,\text{Re}\left(E_j^{t*} E_j^r \frac{1-\exp[-(\mu_{aj}/\sin\psi_d - 2ik'_{z,j})d_j]}{\mu_{aj}/\sin\psi_d - 2ik'_{z,j}} \right) \Bigg\}, \end{aligned} \tag{7}$$

where C_{aj} is the mass fraction of element a in layer j, ρ_j the density of layer j, d_j the thickness of layer j, μ_{aj} the linear absorption coefficient for the fluorescence radiation from element a in layer j, and $k'_{z,j}$ and $k''_{z,j}$ the real and imaginary parts of $k_{z,j}$, i.e., $k_{z,j} = k'_{z,j} - ik''_{z,j}$. The factor A_j results from the integration of the attenuation factor in Eq. (6):

$$A_j = \exp\left[-\sum_{n=1}^{j-1} \frac{\mu_{an} d_n}{\sin\psi_d} \right]. \tag{8}$$

The detection angle ψ_d is usually supposed to be far above the critical angle for total reflection of the outgoing radiation. It is actually set to be 90° for all our ADXRF measurements. This attenuation of the outgoing fluorescence can be ignored when the absorption length for the fluorescent photons $[(\mu_{aj})^{-1}]$ is much larger than the layer thickness d_j, so that $\mu_{aj} d_j \ll 1$ and $e^{-\mu_{aj} d_j} \approx 1$. The last term in Eq. (7) accounts for the interference between transmitted and reflected fields and is responsible for possible oscillations in the fluorescence intensity. The effects of interfacial roughness can be incorporated into the final expression with the Debye-Waller-like exponential factors similar to that discussed in Sec. II A.

For very thin films, the x-ray fluorescence intensity I_{aj} arising from the atoms of a selected element a in layer j can be simplified from Eq. (7) to become[20]

$$I_{aj} \propto \Phi_{aj} d_j |E_j^t + E_j^r|^2 = C_{aj} \rho_j d_j |E_j^t + E_j^r|^2, \quad (9)$$

where Φ_{aj} is the concentration of element a in layer j. The intensity is therefore directly proportional to the total number of atoms per unit area.

C. Numerical calculations and data analysis

The x-ray reflectivity R and the fluorescence intensity I_a for element a given in Eqs. (3) and (7), respectively, can be calculated as functions of the angle θ, and it can also be parametrized with the physical parameters such as mass fraction C_{aj}, mass density ρ_j, roughness σ_j, and thickness d_j, i.e., $R=R(C_{aj},\rho_j,\sigma_j,d_j;\theta)$ and $I_a=I_a(C_{aj},\rho_j,\sigma_j,d_j;\theta)$. The atomic scattering factors are also needed to calculate the optical constants δ and β. Although these two functions contain the same parameters, the functional dependence of x-ray reflectivity on the parameters is quite different from that of x-ray fluorescence intensity. Physically, ADXRF is element specific in the sense that its intensity profile depends on the spatial distribution of the specific element while the x-ray reflectivity is essentially determined by the electron-density profile. In this way the sensitivity of each parameter is so technique dependent that the two different types of measurements can provide different specific informations when averaged over the material structure in the direction perpendicular to the surface. A complete set of parameters such as the layer thickness, interfacial roughness, mass density, and elemental compositions can be deduced from a *simultaneous* analysis of the x-ray reflectivity and ADXRF data by a nonlinear least-squares fitting method. Usually reasonable initial values are chosen for the layer parameters, and these quantities are then consistently adjusted through iterations to reach a minimum of the mean square of differences between the data and the calculated values in the parameter space.

The true reflectivity data are usually obtained with the aid of a longitudinal diffuse scan in order to subtract out the contributions of diffuse scattering. The resultant reflectivity yields the averaged electron-density profile which defines the following parameters for characterizing the geometrical properties of the samples: (i) thickness of the $Si_{1-x}Ge_x$ layer, (ii) interfacial roughness σ_0 between air and the $Si_{1-x}Ge_x$ layer, and (iii) interfacial roughness σ_1 between the $Si_{1-x}Ge_x$ layer and the Si substrate.

The Ge concentration x in the $Si_{1-x}Ge_x$ layer is extracted by analyzing ADXRF data using Eq. (7) and the geometrical parameters obtained from x-ray reflectivity measurements. These input parameters are fixed during our process of curve fitting. The final iterative curve-fitting results through simultaneous analysis of both reflectivity and ADXRF eventually yield a complete set of structural parameters which then serve as the optimized parameters obtained from both reflectivity and ADXRF data for each sample.

Inclusion of an extra layer for possible elemental intermixing at the interface between the $Si_{1-x}Ge_x$ layer and the Si substrate is not necessary in the present case in view of the good simulation results we have obtained as well as the very small interfacial roughness values actually derived from x-ray reflectivity. Therefore, the simultaneous analysis of reflectivity and ADXRF can be performed with great convenience based on a uniform layer of $Si_{1-x}Ge_x$ and a nearly abrupt interface formed between the $Si_{1-x}Ge_x$ alloy and the Si substrate, i.e., a step function is used to represent the Ge concentration profile. Minor intrinsic intermixing at the interface in the present case is naturally accommodated by the small roughness parameter σ_1, and its effects can be neglected in the iterative curve fitting.

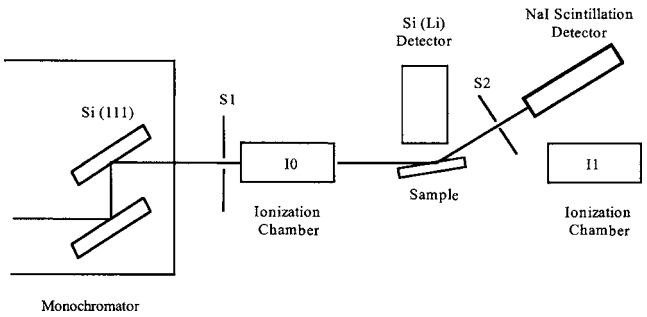

FIG. 2. A schematic diagram of the experimental setup. The energy of incident x rays is selected by a Si (111) double-crystal monochromator. The slit set S_1 defines the horizontal and vertical sizes of the x-ray beam and the slit S_2 defines the resolution of the x-ray reflectivity measurements. The ionization chamber I_0 monitors the intensity of the incident x-ray beam and another ionization chamber I_1 is used to align the sample.

III. EXPERIMENT

Epilayers of $Si_{1-x}Ge_x$ were grown on Si(100) substrates using the MBE technique. A thick (about 1000 Å) Si buffer layer was first deposited on a Si(100) substrate before growing the $Si_{1-x}Ge_x$ epilayers. The nominal concentration x of Ge was varied from 0.2 to 0.9 with a step of 0.1 during the MBE growth at temperatures around 500 °C with a pressure of about 4×10^{-9} torr. The nominal layer thickness for all the samples was controlled to be around 150 Å.

The x-ray measurements were carried out at Beamline X3B1 at the National Synchrotron Light Source (NSLS) in Brookhaven National Laboratory (BNL). The experimental setup for x-ray reflectivity and ADXRF measurements is shown schematically in Fig. 2. The x-ray beam from the storage ring is monochromatized by a Si(111) double crystal and collimated by a set of slits S_1. The beam size is set to be approximately 0.1×5 mm.[2] The intensity of the incident x-ray beam is monitored by an ionization chamber I_0. The fluorescence intensity is measured by an energy-dispersive solid-state Si(Li) detector placed a few millimeters above the sample. The scattered intensity of x-ray reflectivity is measured by a NaI scintillation detector with a set of slits S_2 in front of it to define the angular resolution. The sample and the detector are mounted on a two-circle goniometer whose rotation is controlled by a computer with 0.001° step precision. An incident photon energy of 11.0 keV was used for the x-ray reflectivity experiments while the ADXRF measurements were performed with an x-ray energy of 12.0 keV to excite the germanium atoms in the SiGe epilayers (Ge K edge =11.103 keV).

IV. RESULTS AND DISCUSSION

Measured reflectivity data (open circles) and theoretical calculations (solid lines) are shown in Fig. 3 for all the

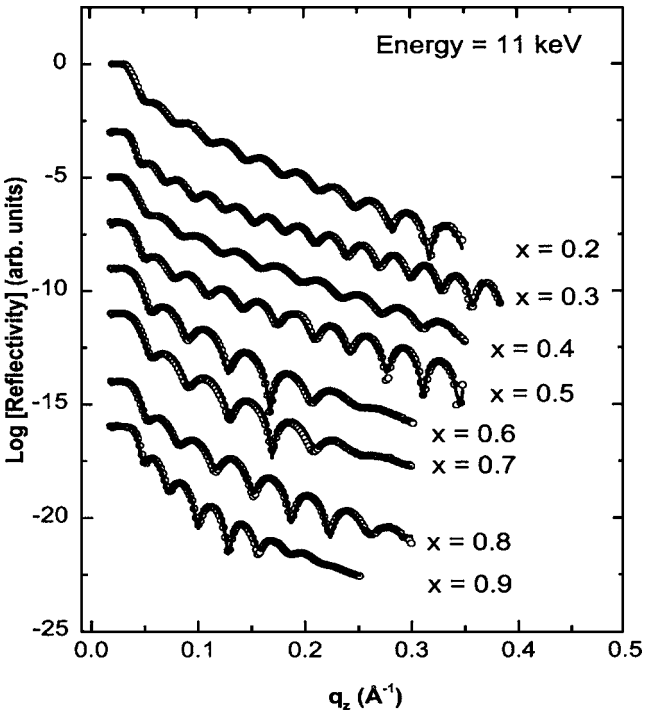

FIG. 3. True specular reflectivity data (open circles) and theoretical calculations (solid lines) for all the SiGe epilayer samples studied. The data are obtained by subtracting out the longitudinal diffuse scattering background with an angle offset of $\delta\theta=0.1°$ taken at an x-ray energy 11 keV. Geometrical parameters are extracted through theoretical calculations using Eq. (3). x is the nominal content of Ge estimated at epitaxial growth, subject to correction after ADXRF analysis.

samples studied in the present experiment. The experimental data are the true specular reflectivity after subtracting out the longitudinal diffuse scattering obtained with an angle offset of $\delta\theta=0.1°$. The agreement between the experimental results and theoretical calculations is very good. There are oscillations (Kiessig fringes) with a single frequency arising from the interference of x rays reflected from the top surface and the SiGe/Si interface. The oscillation frequency is primarily determined by the thickness of the SiGe layer and the amplitude is mainly affected by the optical contrast (mismatch of optical constants between the SiGe layer and the Si substrate) and roughness of the interface as well as the top surface. As expected, the overall oscillation amplitude in Fig. 3 varies with the Ge concentration. Even without any detailed analysis, this behavior can be qualitatively understood in terms of the optical contrast because more Ge in the SiGe layer gives higher optical contrast with respect to the Si substrate. The numerical results are summarized in Table I. The thickness of the SiGe layers was found to vary from 150 to 210 Å, close to the nominal value set during the MBE growth. The roughness for the top surface ranges from 6 to 15 Å and that for the SiGe/Si interface 5 to 8 Å, indicating that the SiGe/Si interfaces are reasonably smooth and all are well defined. The sensitivity of this technique for the determination of thickness and roughness is quite high, with uncertainties of approximately 4 and 1 Å, respectively. This supports the previous statement that the x-ray reflectivity technique is very sensitive to the geometrical parameters.

A typical angular dependence of Ge $K\alpha$ fluorescence intensity for the sample with a nominal value of $x=0.8$ is shown in Fig. 4: the open circles are raw data and the solid line is the theoretical calculation based on Eq. (7). The intensity of Ge $K\alpha$ radiation at 9.886 keV was recorded as a function of the grazing incidence angle. For grazing incidence lower than the critical angle of the SiGe layer, x rays are totally reflected, only the evanescent fields penetrate into the layer which is optically less dense than air in the x-ray wavelength regime, and the fluorescence intensity is very small. With an increase of the grazing incidence angle, there is an abrupt increase in the fluorescence intensity around the critical angle, and then the intensity decreases and stays at a certain level for grazing angles greater than the critical angle. There may be oscillations in some materials depending on the optical contrast and thickness. All these features can be quantitatively understood in terms of the interaction of x rays with thin layer materials.

TABLE I. Thickness and interfacial roughness of the samples obtained by comparison of experimental data with theoretical calculations; x is the nominal concentration of Ge in the SiGe epilayer, D the thickness of SiGe layer, σ_0 the roughness of the top surface, and σ_1 the roughness between the SiGe layer and the Si substrate.

Sample	D(Å)	σ_0(Å)	σ_1(Å)
$x=0.2$	179±2	8±1	5±1
$x=0.3$	212±3	6±1	5±1
$x=0.4$	163±4	7±1	6±1
$x=0.5$	183±2	7±1	5±1
$x=0.6$	154±2	11±1	6±1
$x=0.7$	152±2	11±1	6±1
$x=0.8$	171±2	10±1	6±1
$x=0.9$	206±5	15±1	8±1

In the theoretical calculation of x-ray fluorescence, we have used the values of layer thickness and interfacial roughness obtained from the reflectivity data. As mentioned before, we have also assumed a step function for the Ge depth

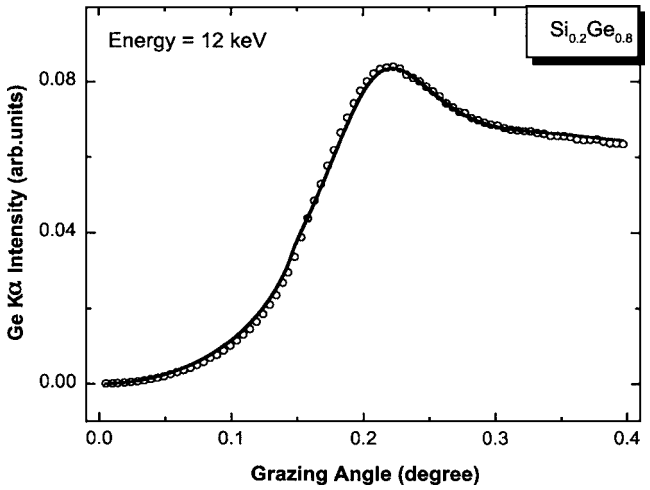

FIG. 4. A typical ADXRF profile for $Si_{1-x}Ge_x/Si$ with a nominal Ge content of $x=0.8$ obtained with an x-ray energy of 12 keV (open circles) and theoretical calculation (solid line). The x-ray fluorescence intensity shows typical features of a thin film. A true Ge concentration is deduced by analyzing the data using Eq. (7) while the geometrical parameters obtained from the x-ray reflectivity data are kept fixed.

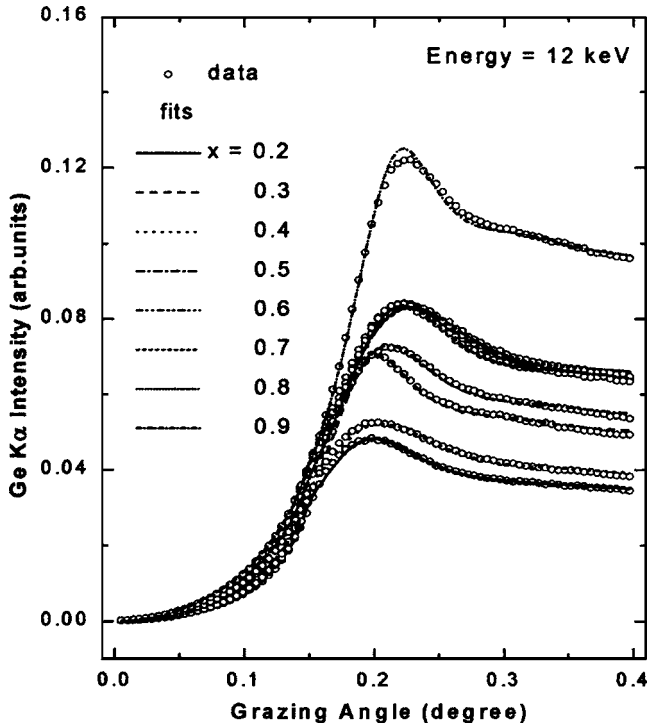

FIG. 5. Measured ADXRF data (open circles) and theoretical calculations (lines) for all the SiGe epilayers. x is the nominal content of Ge estimated at epitaxial growth, subject to correction after ADXRF analysis. The x-ray fluorescence intensity obeys an approximation $I_{\mathrm{Ge}} \approx C_{\mathrm{Ge}} \rho d$. A complete set of structural parameters is obtained from the analysis of the ADXRF data along with the geometrical parameters determined from x-ray reflectivity analysis.

profile for ADXRF analysis in view of the measured small roughness of the SiGe/Si interface. In this way the geometrical layer parameters such as thickness and roughness were both fixed in the ADXRF curve-fitting process and a uniform distribution of the SiGe epilayer was justified. The experimental data are in very good agreement with the theoretical calculation. The Ge concentration determined from the ADXRF result is 57% (x=0.57), which is quite different from the nominal Ge content 0.8 based on a rough estimate by timing during the epitaxial growth. This result thus demonstrates that ADXRF can serve as an effective tool to *calibrate* the content of a specific component in a composite thin-film material.

In addition to the correction for the sample with a nominal value of x=0.8 by ADXRF calibration, we have also corrected for the actual Ge contents in other samples, including those with nominal x values of 0.3, 0.6, and 0.7. The ADXRF data and theoretical calculations for all the samples studied are shown in Fig. 5. The numerical results are listed in Table II. It can be seen that the fluorescence intensity obeys an approximation $I_{\mathrm{Ge}} \approx C_{\mathrm{Ge}} \rho d$ in Eq. (9), where C_{Ge} is the Ge concentration, ρ the density, and d the thickness of the SiGe layer. The results after ADXRF correction are all consistent with our x-ray-diffraction measurements.

We have also deduced the real and imaginary parts δ and β of the complex refractive index for each sample using the x-ray reflectivity and ADXRF results. Since x-ray reflectivity is mainly governed by the electron density, the optical constant δ plays a more important role in controlling the x-ray

TABLE II. Ge concentration in the SiGe epilayers obtained from the analysis of the ADXRF data; x is the nominal concentration of Ge in the SiGe epilayers.

Sample	Measured concentration
x=0.2	0.27±0.02
x=0.3	0.35±0.02
x=0.4	0.34±0.02
x=0.5	0.46±0.02
x=0.6	0.71±0.04
x=0.7	0.70±0.02
x=0.8	0.57±0.03
x=0.9	0.83±0.04

reflectivity than β. The values of δ at 11 keV for bulk Si and Ge are 4.04×10^{-6} and 6.74×10^{-6}, respectively, hence the optical constant δ for the $Si_{1-x}Ge_x$ epilayers is expected to be a monotonically increasing function of Ge concentration x according to the additive law, i.e., $\delta = C_{\mathrm{Si}}\delta_{\mathrm{Si}} + C_{\mathrm{Ge}}\delta_{\mathrm{Ge}}$ (C_{Si} and C_{Ge} are the mass fractions of Si and Ge in the SiGe layer). In Fig. 6(a), the optical constant δ for the SiGe layers is plotted as a function of the nominal Ge concentration (-○-) and also against the corrected Ge concentration from the ADXRF analysis (-■-). The plot against the Ge concentration obtained from the ADXRF analysis shows a more reasonable monotonic behavior. A similar plot of β is shown in Fig. 6(b). These results help to demonstrate that the ADXRF technique is very useful for the calibration of Ge concentration in the $Si_{1-x}Ge_x$ epilayer system.

X-ray-diffraction measurements at 11 keV were carried

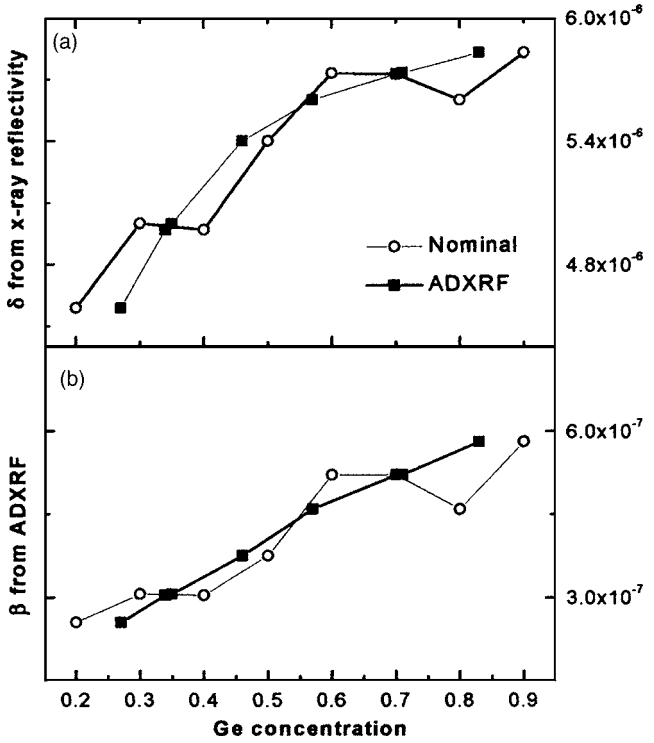

FIG. 6. (a) Optical constant δ of the SiGe layers obtained from the x-ray reflectivity analysis vs Ge content: the nominal concentration (-○-) and the measured concentration from the ADXRF analysis (-■-). (b) Optical constant β of the SiGe layers obtained from the ADXRF analysis vs Ge content as in (a).

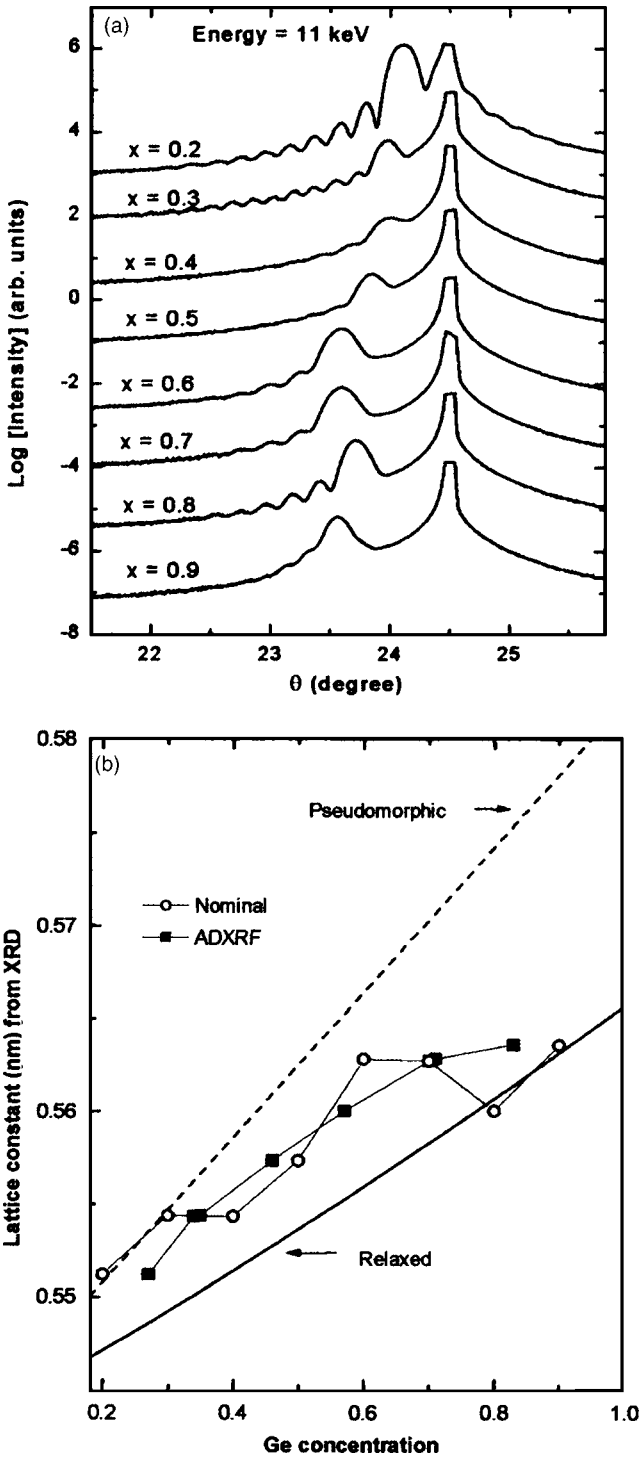

FIG. 7. (a) X-ray-diffraction data taken with 11 keV for determining the lattice constants in the vertical direction of the SiGe layers. (b) Lattice constant vs Ge content: the nominal concentration (-○-) and the measured concentration from the ADXRF analysis (-■-). The two straight lines serve as guides for the extreme cases of pseudomorphic growth of SiGe on Si and completely relaxed SiGe random alloys.

out to determine the lattice constant of the SiGe layers in the vertical direction, and the results obtained around the Si (004) peak are shown in Fig. 7(a). The narrow and sharp peak at a higher angle is due to the substrate Si (004) plane and the broad peaks at lower angles arise from the SiGe layers. This indicates that the lattice spacing of the SiGe layer in the vertical direction is larger than that of the substrate. The lattice constants extracted from the diffraction data are listed in Table III. The lattice constant of SiGe alloys is anticipated to increase with the Ge concentration, and this is borne out in our experiments. In Fig. 7(b), the lattice constants obtained from x-ray diffraction are plotted as functions of the nominal Ge concentration (-○-) as well as the Ge concentration deduced from the ADXRF analysis (-■-). Once again, the smooth variation of lattice constant lends more support to the reliability of concentration calibration with the ADXRF method. The two straight lines serve as guides for the extreme cases of pseudomorphic growth of SiGe on Si and completely relaxed random alloys (Vegard's law). The actual lattice constant of the $Si_{1-x}Ge_x$ system naturally depends on the strain due to lattice mismatch between Si and Ge and the growth conditions. This plot also shows the importance of ADXRF corrections for the Ge concentration in the alloy films in order to reliably differentiate the system between pseudomorphic growth and complete relaxation.

TABLE III. Lattice constant of the SiGe epilayers obtained from the x-ray-diffraction data; a is lattice constant in the vertical direction of the SiGe layers. The uncertainty estimation for the determination of lattice constant for all the samples is ~0.002 Å.

Sample	a(Å)
x=0.2	5.512
x=0.3	5.544
x=0.4	5.544
x=0.5	5.574
x=0.6	5.628
x=0.7	5.627
x=0.8	5.600
x=0.9	5.636

The results shown in Fig. 7(b) indicate that the SiGe alloys are neither fully relaxed nor pseudomorphic. The lattice constant shows a trend to approach the limit of relaxed random alloys as the Ge concentration increases. The variation of lattice constant with Ge concentration may also be due to a complex functional dependence of the critical thickness on the Ge content and growth conditions.

V. CONCLUSION

In the present experiment, the x-ray reflectivity and ADXRF techniques have been demonstrated as useful nondestructive methods to characterize layer-structured materials. These methods have been applied to a study of a series of $Si_{1-x}Ge_x$ epilayers to determine the actual Ge concentration as well as the layer thickness and interfacial roughness. The x-ray reflectivity technique has shown high sensitivity for the determination of geometrical quantities such as thickness and interfacial roughness. The ADXRF technique has been demonstrated as an efficient *element-specific* tool for investigating the concentration of selected atomic species in a composite system. Our results also demonstrate that the ADXRF method can be used as an effective tool for calibrating the postgrowth Ge concentration in the alloys, in particular, the thin-film systems.

The present research is supported in part by the U.S. Department of Energy.

[1]S. Kim, Y. L. Soo, G. Kioseoglou, Y. H. Kao, and A. D. Compaan, J. Appl. Phys. **96**, 1007 (2004).
[2]S. Kim, Y. L. Soo, G. Kioseoglou, Y. H. Kao, K. Ramanathan, and S. K. Deb, J. Appl. Phys. **91**, 6416 (2002).
[3]J. P. Dismukes, L. Ekstrom, and R. J. Paff, J. Phys. Chem. **68**, 3021 (1964).
[4]E. R. Johnson and S. M. Christian, Phys. Rev. **95**, 560 (1954).
[5]G. Margaritondo, Surf. Sci. **168**, 439 (1986).
[6]J. C. Bean, L. C. Feldman, A. T. Fiory, S. Nakahara, and I. K. Robinson, J. Vac. Sci. Technol. A **2**, 436 (1984).
[7]R. People and J. C. Bean, Appl. Phys. Lett. **47**, 322 (1985).
[8]J. Huang, Z. Ye, H. Lu, and D. Que, J. Appl. Phys. **83**, 171 (1998).
[9]J.-M. Baribeau and H. Lafontaine, Thin Solid Films **321**, 141 (1998).
[10]J. C. Woicik *et al.*, Phys. Rev. B **43**, 2419 (1991).
[11]H. Kajiyama, S. Muramatsu, T. Shimada, and Y. Nishino, Phys. Rev. B **45**, 14 005 (1992).
[12]D. B. Aldrich, R. J. Nemanich, and D. E. Sayers, Phys. Rev. B **50**, 015026 (1994).
[13]J. C. Aubry, T. Tyliszczak, A. P. Hitchcock, J.-M. Baribeau, and T. E. Jackman, Phys. Rev. B **59**, 12 872 (1999).
[14]D. E. Jesson, S. J. Pennycook, and J. M. Baribeau, Phys. Rev. Lett. **66**, 750 (1991).
[15]J.-H. Cho, S. Jeong, and M. H. Kang, Phys. Rev. B **50**, 17 139 (1994).
[16]L. Patthey, E. L. Bullock, T. Abukawa, S. Kono, and L. S. O. Johansson, Phys. Rev. Lett. **75**, 2538 (1995).
[17]L. Vegard, Z. Phys. **5**, 17 (1921).
[18]J. C. Bean, J. Cryst. Growth **70**, 444 (1984).
[19]D. C. Houghton, C. J. Gibbings, C. G. Tuppen, M. H. Lyons, and M. A. G. Halliwell, Appl. Phys. Lett. **56**, 460 (1990).
[20]D. K. G. de Boer, Phys. Rev. B **44**, 498 (1991).
[21]U. Weisbrod, R. Gutschke, J. Knoth, and H. Schwenke, Appl. Phys. A: Mater. Sci. Process. 53, 449 (1991).
[22]A. Król, C. J. Sher, and Y. H. Kao, Phys. Rev. B **38**, 8579 (1988).
[23]W. W. van den Hoogenhof and D. K. G de Boer, Spectrochim. Acta, Part B **48**, 277 (1993).
[24]L. G. Parratt, Phys. Rev. **95**, 359 (1954).
[25]M. Born and E. Wolf, *Principles of Optics*, 5th ed. (Pergamon, Oxford, 1975).
[26]L. Névot and P. Croce, Rev. Phys. Appl. **15**, 761 (1980).
[27]D. Bahr, W. Press, R. Jebasinski, and S. Mantl, Phys. Rev. B **47**, 4385 (1993).
[28]B. Vidal and P. Vincent, Appl. Opt. **23**, 1794 (1984).
[29]B. Pardo, T. Megademini, and J. M. André, Rev. Phys. Appl. **23**, 1579 (1988).
[30]D. K. G. de Boer and W. W. van den Hoogenhof, Spectrochim. Acta, Part B **46**, 1323 (1991).
[31]R. Klockenkämper, *Total Reflection X-ray Fluorescence Analysis* (Wiley, New York, 1997), p. 84.